ESA Climate Change Initiative
aerosol_cci

Algorithm Theoretical Basis Document (ATBD)
Instruments: ATSR-2 and AATSR
Algorithm: SU-ATSR

Version 4.3

DOCUMENT STATUS SHEET

	FUNCTION	NAME	DATE	SIGNATURE
LEAD AUTHOR	editor	Peter North	10/9/2012	
CONTRIBUTING AUTHORS	Algorithm development Algorithm development Algorithm development Algorithm development	Andreas Heckel Will Davies Suzanne Bevan Will Grey	10/9/2012 10/9/2012 1/2/2012 1/9/011	
REVIEWED BY	Co-science leader	Gerrit de Leeuw		
APPROVED BY	Technical officer (ESA)			
ISSUED BY	Project manager			

EXECUTIVE SUMMARY

The SU-ATSR algorithm has been developed at Swansea University for estimation of atmospheric aerosol and surface reflectance for the ATSR-2 and AATSR sensors. Over land, the algorithm employs a parameterised model of the surface angular anisotropy, and uses the dual-view capability of the instrument to allow estimation without a priori assumptions on surface spectral reflectance. Over ocean, the algorithm uses a simple model to exploit the low ocean leaving radiance at red and infra-red channels at both nadir and along-track view angles. While previous versions of the algorithm haves been described in depth in previous publications, a number of innovations are documented here developed under the aerosol CCI project. Developments under the Aerosol CCI programme include (i) enhanced treatment of aerosol mixtures, (ii) inclusion of a model of ocean surface including wind-speed and pigment dependency, and (iii) analytical propagation of uncertainty. This ATBD summarises the underlying principles, equations input/output and implementation details of the algorithm, based on the algorithm version 4.3.

Issue	Date	Modified Items / Reason for Change
1.0	4/3/2011	First edition
2.0	10/9/12	Major revision, to document developments under the Aerosol CCI project: Section 4.1 Surface treatment. New ocean model based on Aerosol_cci recommendations Section 5.1 Cloud screening and preprocessing. Options added to use alternative cloud masks. Section 5.2: Aerosol model and climatology. Upgraded algorithm now uses common aerosol model set, and allows continuous variation of aerosol properties based on mixtures of these, and use of climatology of composition as a prior. Section 8: Error budget estimates. New analytic error propagation equations.
3.0	15/6/2017	Revision to reflect changes up to current version SU 4.3, which concern refinements to operational implementation (section 5) Section 5.1 new section with added development and detail on super-pixel aggregation Section 5.3 Aerosol climatology added explaining definition and use of aerosol climatology in inversion Section 5.5 Inversion procedure modified and expanded to include detail on constraints on the inversion, including introduction of 'smoothness' constraint between super-pixels Section 5.6 added detailing post-processing for cloud contamination reduction

LIST OF TABLES

LIST OF FIGURES

TABLE OF CONTENTS

1 INTRODUCTION

This document describes the theoretical basis for the aerosol retrieval algorithm developed for ATSR-2 and AATSR by Swansea University This algorithm is referred to as SU-ATSR, with current version v4.3.

The SU-ATSR algorithm has been extensively described in a series of peer-reviewed papers [references listed by number in section 1.2.2] and reports [references listed by number in section 1.2.2]. This ATBD aims to provide an overview of the algorithm with detailed references to the above-mentioned papers and reports, with summaries of the issues that are important for the aerosol-cci work, and developments to the algorithm made within the CCI project.

1.1 References

1.1.1 Applicable Documents

[AD1] Statement of Work "ESA Climate Change Initiative Stage 1, Scientific user Consultation and Detailed Specification", ref EOP-SEP/SOW/0031-09/SP. Issue 1.4, revision 1, dated 9 November, 2009, together with its Annex C "Aerosols" (altogether the SoW).

[AD2] The Prime Contractor's Baseline proposal, ref. 3003432, Revision 1.0, dated 16 June 2010, and the minutes of the July 26, 2010 kick-off meeting.

[AD3] Aerosol-cci project management plan (PMP), version 1.3.

1.1.2 Reference Documents

[RD1] Bevan, S.L., North, P.R.J., Grey, W.M.F., Los, S.O. and Plummer, S.E. (2009), Impact of atmospheric aerosol from biomass burning on Amazon dry-season drought. Journal of Geophysical Research, **114**, D09204, doi:10.1029/2008JD011112.

[RD2] Bevan, S.L., North, P.R.J., Los, S.O. and Grey, W.M.F. (2012). A global dataset of atmospheric aerosol optical depth and surface reflectance from AATSR. Remote Sensing of Environment, 116, 119-210.

[RD3] Davies, W.H., North, P.R.J., Grey, W.M.F. and Barnsley, M.J. (2010), Improvements in Aerosol Optical Depth Estimation using Multi-angle CHRIS/PROBA Images, *IEEE Transactions on Geoscience and Remote Sensing,* **48**(1), 18-24.

[RD4] Grey., W.M.F., North., P.R.J., Los, S.O., and Mitchell, R.M., (2006). Aerosol optical depth and land surface reflectance from multi-angle AATSR measurements: Global validation and inter-sensor comparisons. *IEEE Transactions on Geoscience and Remote Sensing,* **44(8)**, 2184 – 2197.

[RD5] Grey., W.M.F, North., P.R.J., and Los, S. (2006b). Computationally efficient method for retrieving aerosol optical depth from ATSR-2 and AATSR data, *App. Optics*, **45(12):** 2786-2795.

[RD6] North, P.R.J., Briggs, S.A., Plummer, S.E. and Settle, J.J., (1999). Retrieval of land surface bidirectional reflectance and aerosol opacity from ATSR-2 multi-angle imagery, *IEEE Transactions on Geoscience and Remote Sensing*, **37(1),** 526-537.

[RD7] North, P. R. J. (2002). Estimation of aerosol opacity and land surface bidirectional reflectance from ATSR-2 dual-angle imagery: Operational method and validation, *J. Geophys. Res*., **107**, doi:10.1029/2000JD000,207.

[RD8] North, P.R.J., Brockmann , C., Fischer, J., Gomez-Chova, L., Grey, W., Heckel, A., Moreno, J., Preusker, R. and Regner, P. (2008). MERIS/AATSR synergy algorithms for cloud screening, aerosol retrieval and atmospheric correction. *In Proc. 2nd MERIS/AATSR User Workshop, ESRIN, Frascati, 22- 26 September 2008.* (CD-ROM), ESA SP-666, ESA Publications Division, European Space Agency, Noordwijk, The Netherlands.

[RD9] *ESA Climate Change Initiative Aerosol_cci, Technical note: Aerosol models*. Version 1.1, G. de Leeuw (Ed)., 2011.

2 INSTRUMENT CHARACTERISTICS

The AATSR instrument is a scanning radiometer, sensing at thermal infrared, reflected infra-red and visible wavelengths with two ~500 km wide conical swaths, with 555 pixels across the nadir swath and 371 pixels across the forward swath. The specifications of AATSR and ATSR-2 are the same, except that the ATSR-2 instrument employed a reduced swath of visible channels over and near oceans due to data transmission restrictions. The set of channels are listed in Table 2-1. The nominal pixel size is 1 km^2 at the center of the nadir swath and 1.5 km^2 at the center of the forward swath. For the AATSR level 1 products the forward pixels are sampled to 1km in order to be the same size as the nadir pixels. The conical scan provides two views of the surface and improves the capacity for atmospheric correction and enables observations of the ocean surface under a solar zenith angle of ~55° in the forward direction. The channels at 1.6µm and 0.87µm are especially important to correct for the impact of aerosols, especially above coastal waters, since at this spectral range there is nearly no backscattering of solar radiation emanating from the water body. For land aerosol retrieval, the bands at shorter wavelengths (550nm and 665nm) where aerosol scattering is greater with respect to surface scattering are important.

Table 2-1: AATSR spectral channels

Channel	Wave-length (nm)	Band-width (nm)
1	550	20
2	665	20
3	865	20
4	1610	60
5	3740	380
6	10850	90
7	12000	1000

3 SCOPE OF THE PROBLEM

Here we introduce the background and motivation to the algorithm, which exploits the ATSR dual angle for retrieval of aerosol optical thickness and type over both land and ocean

3.1 Aerosol optical thickness and scattering properties

.The parameters required to model aerosol radiative effects are aerosol optical depth (AOT) for a given reference wavelength, its spectral dependence, which may be approximated by the Angstrom coefficient, single scattering albedo, and phase function. These properties are closely related to aerosol amount, composition and size distribution. The net effect of aerosol on climate forcing depends on its optical properties (absorption and scattering). To date, most retrieval schemes return spatially varying estimates of AOT as the main parameter, and some additionally return information on aerosol size distribution (e.g. Remer et al., 2005) or the related property of Angstrom coefficient (e.g. Veefkind et al 1999). Recent methods have explored search for the most probable candidate aerosol model from a limited database, based on fit to the observations, with further aerosol properties defined by this model (North 2002b; Holzer-Popp et al., 2008; Diner et al., 2009).

In general, it is more challenging to retrieve required aerosol properties over the land than the ocean. This is because the scattering from the land surface tends to dominate the satellite signal making it difficult to discern the atmospheric scattering contribution, particularly over bright surfaces. In addition, obtaining an accurate model of the land surface is further complicated because bi-directional reflectance is highly variable, both spatially and temporally.

3.2 Satellite retrieval methods

3.2.1 Single-view methods

- Most currently available aerosol retrievals are based on data from instruments with a single sampling of the angular domain. These algorithms are based on different assumptions, depending on available spectral sampling. In general the retrievals need to use known wavelength dependence of surface reflectance in order to provide information on the aerosol. The separation of the surface contribution is always based on a priori knowledge about the spectral properties of the surface.

3.2.2 Multiple view-angle (MVA) methods

While spectral methods may produce very good results in regions where the assumptions are fulfilled, global aerosol retrievals show a number of uncertainties due to the large variability in spectral surface properties. Use of multiple view-angle imagery allows an additional

constraint to be placed, since the same area of surface is viewed through different atmospheric path lengths. The concept was pioneered by ATSR on ERS-2, originally for atmospheric correction of SST for the effects of water vapour (Barton et al., 1989). In addition, there is scope to use the increased angular sampling of the land surface to further constrain retrieval of albedo and vegetation biophysical parameters (Diner et al., 1999). Several instruments have been designed to exploit the ability of MVA techniques for aerosol retrieval, including MISR, using 9 cameras tilted at angles in the range ± 70.5° along-track, and POLDER, which employs a CCD array to sample continuousl9 at ± 43° along-track (Martonchik et al., 1998; Leroy et al., 1997).

For the ATSR instrument series, 2 view directions are available, at approximately nadir and 55° along-track requires an approach which exploits the similarity of the surface anisotropy across wavelengths. This is due to the fact the anisotropy is dominated by geometric shadowing effects, which are wavelength invariant. However other effects contribute to anisotropy; the differential viewing of canopy/understory surfaces with view angle, and the degree of multiple scattering, which tends to reduce anisotropy over bright surfaces. A simple approximation assuming spectral invariance of the BRDF (Mackay et al., 1999; Flowerdew and Haigh, 1996) has been used in inversion schemes (Veefkind et al., 2000) to provide a successful retrieval of aerosol. The method has developed further to include enhanced modelling of the spectral variation of anisotropy (North et al., 1999) to give an operational method from which global retrieval of aerosol properties has been achieved using the ESA Grid Processing on Demand (GPOD) system (North 2002b; Grey et al., 2006a,b). Validation by comparison with AERONET shows robust retrieval over all land surfaces, including deserts (Grey et al., 2006b; Bevan et al., 2009). The method has also recently been applied to estimation of aerosol from the CHRIS PROBA instrument, by exploiting the ability of the instrument to acquire 5 views of the target by satellite pointing (Davies et al., 2010), and in formation of anticipated aerosol products for Sentinel-3 (e.g. Davies et al., 2015, Sobrino et al., 2016). The use of a cross-spectral constraint on surface anisotropy has also recently been incorporated into the MSR processing algorithm (Diner et al., 2005).

The principal advantage of an MVA approach is that no *a priori* information of the surface spectrum is required and aerosol properties can be retrieved over all surface types, including bright deserts. Limitations of the angular approach are that the algorithms require accurate co-registration of the images acquired from multiple view angles. Normally aerosol is retrieved at a lower resolution than the pixel resolution, to decrease the effect of misregistration errors, for example at 18km for MISR and 8km for ATSR (Diner et al., 2009; North et al., 2002b), and the methods may be sensitive to undetected sub-pixel clouds (North et al., 1999).

4 SCIENTIFIC BACKBROUND

The algorithm uses an iterative optimisation to determine values of atmospheric optical thickness and aerosol type. The optimisation uses a parameterised model of either land or ocean. The method is described in detail in [RD1-RD6]. Here we outline the theory behind the inversion, comprising modelling reflectance over land and ocean, approximation of atmospheric scattering and numerical inversion. Developments under the Aerosol CCI programme include (i) enhanced treatment of aerosol mixtures, (ii) inclusion of a model of ocean surface including wind-speed and pigment dependency, and (iii) analytical propagation of uncertainty.

4.1 Surface treatment

4.1.1 Land surface

The surface model is based on a physical model of light scattering which constrains the variation of angular anisotropy (North et al 1999). It is applicable for simultaneous estimation of AOD and surface reflectance for data where at least two view angles are available, such as the AATSR (North et al., 1999; North 2002; Grey et al., 2006a,b). Methods employing similar principals have also been developed for AATSR and other multi-view sensors, (Veefkind et al., 1999; Diner et al., 2005; Kokhanovsky et al., 2007). The principal advantage of this approach is that no *a priori* information of the surface is required and aerosol properties can be retrieved even over bright surfaces. The model accounts for some spectral variation of the angular shape owing to the variation of the diffuse fraction of light with wavelength. The surface anisotropy is reduced when the diffuse irradiance is high because the contrast between shadowed and sunlit surfaces decreases. Anisotropy is similarly dependent for bright targets owing to the multiple-scattering of light between the surface elements. The atmospheric scattering elements including aerosols and gas molecules are comparable in size to the wavelength of light at optical wavelengths. As a result, the effect of atmospheric scattering on the anisotropy will be a function of wavelength and the shape of the BRDF will vary. Taking these effects into account results is a physical model of spectral change with view angle (North et al., 1999):

$$\rho_{ang\_\mathrm{mod}}(\lambda,\Omega) = (1-D(\lambda))v(\Omega)w(\lambda) + \frac{\gamma w(\lambda)}{1-g}\left[D(\lambda) + g(1-D(\lambda))\right] \qquad (1)$$

where $g = 1 - \gamma\omega(\lambda)$, λ is the wavelength, Ω is the viewing geometry (forward or nadir view in the cases of AATSR), ρ_{ang_mod} is the modelled bidirectional reflectance, γ is the fraction contributing to higher-order scattering and is fixed at 0.3, and D is the fraction of diffuse irradiance. The model separates the angular effects of the surface into two components, a structural parameter v that is dependent only on the viewing and illumination geometry, and the spectral parameter ω, that is dependent only on the wavelength. The free parameters that we need to retrieve through model inversion are $w(\lambda)$ and $v(\Omega)$. The angular

reflectance of a wide variety of natural land surfaces fits this simple model. In contrast, reflectance that is a mixture of atmospheric and surface scattering does not fit this model well. The fitting error of surface data to the model gives an estimate of the degree of atmospheric contamination for a particular set of reflectance measurements and allows us to find the atmospheric parameters which allow retrieval of a realistic surface reflectance.

4.1.2 Ocean surface

Over ocean aerosol is retrieved by inversion of dual-angle measurements using a model of ocean surface reflectance. The retrieval is performed where both views are cloud-free and excluding regions of sunglint defined by flags supplied with the AATSR product. A surface model (Koepke, 1984) is used to give an estimate of ocean surface BRDF:

$$\rho_{ocean\_\mathrm{mod}} = \rho_{wc} + (1 - f_W)\rho_{gl} + (1 - \rho_{wc})\rho_{sw} \qquad (2)$$

where ρ_{wc} denotes reflectance due to whitecaps , f_W is the fraction of surface covered in whitecaps, ρ_{gl} is the glint reflectance and ρ_{sw} is the water reflectance.

The terms are computed using the models of Cox and Munk (1954) for glint, Monahan & O'Muircheartaigh (1980) and Koepke (1984) for foam fraction and spectral reflectance, and Morel's case I water reflectance model dependent on pigment concentration (Morel 1988). The model is run coupled with the 6SV atmospheric model to account for sky glint.

Inputs required *a priori* are surface wind speed W (ms^{-1}) and pigment concentration C (mg m^{-3}). In the current implementation fixed values of 3 ms^{-1} for wind speed and 0.1 mg m^{-3} for chlorophyll concentration are used as default.

4.2 Atmospheric radiative transfer approximation

For a given sensor waveband, and atmospheric profile, the relationship between surface directional reflectance R_{surf} top of atmosphere reflectance R_{TOA} can be approximated by the equation:

$$R_{TOA}(\theta_v,\theta_s,\phi) = [R_{atm}(\theta_v,\theta_s,\phi) + T(\theta_s)T(\theta_v)\frac{R_{surf}(\theta_v,\theta_s,\phi)}{1-\rho_{atm}R'_{surf}}] \qquad (3)$$

where R_{atm} denotes the atmospheric scattering term (TOA reflectance for zero surface reflectance), T denotes atmospheric transmission for either sensor to ground or ground to sensor, and R_{atm} denotes atmospheric bi-hemispherical albedo. The term R'_{surf} denotes ground reflectance for multiple scattered light, and here we use the approximation $R'_{surf} = R_{surf}$.

By rearranging (3), the quantity R_{surf} can readily be derived from R_{TOA} by

$$R_{surf}(\theta_v,\theta_s,\phi) = \frac{f}{1+\rho_{atm}f} \tag{4}$$

where

$$f = \frac{R_{TOA}(\theta_v,\theta_s,\phi) - R_{atm}(\theta_v,\theta_s,\phi)}{T(\theta_s)T(\theta_v)} \tag{5}$$

This procedure provides an atmospherically corrected surface directional reflectance (SDR), also referred to as Lambert equivalent reflectance (LER) or bidirectional reflectance factor (BRF). Note that different values of SDR will be retrieved for different view directions.

The calculation is made efficient by pre-compilation of look-up tables for the coefficients defined for each waveband accounting for the spectral response functions Grey et al 2006, using the Vector 6S radiative transfer model (Vermote et al (1997), Kotchenova et al. (2007)), which accounts for polarisation. Although observations at differing view angles will recover a differing surface reflectance value, the surface is approximated as Lambertian for the calculation of multiple scattering terms.

4.3 Parameter estimation

A set of surface reflectances are calculated for a given atmospheric aerosol model and AOD parameterised by value at 550 nm. An error metric is defined on the surface reflectance set based on a weighted fit to either land or ocean models:

$$E_{\text{mod}} = \sum_{\Omega=1}^{2}\sum_{\lambda=1}^{4} W_{\lambda,\Omega}\left[\rho_{surf}(\lambda,\Omega) - \rho_{ang\_\text{mod}}(\lambda,\Omega)\right]^2 \tag{6}$$

$$E_{\text{mod}} = \sum_{\Omega=1}^{2}\sum_{\lambda=2}^{4} W_{\lambda,\Omega}\left[\rho_{surf}(\lambda,\Omega) - \rho_{ocean\_\text{mod}}(\lambda,\Omega)\right]^2 \tag{7}$$

where ρ_{ocean_mod} and ρ_{ang_mod} are the surface reflectances estimated using the equations for ocean and land respectively. For ρ_{ang_mod} the value is based on the best-fit values of the free parameters. The weight vectors are defined by estimated uncertainty in observation and model, discussed in section 8, where error estimates for retrieved parameters are also given. The algorithm proceeds with the same inversion framework and aerosol model set as for land surface retrieval but the angular model constraint is simply replaced by a simple metric of fit on the ocean reflectance model. To identify the best aerosol model from the candidate model set, the algorithm is run to find estimates of AOD for all models, and a single optimal model selected based on goodness of fit from to the land or ocean model.

5 IMPLEMENTATION

In this section we give the detail of practical implementation of the theory discussed in section 4 for aerosol retrieval.

5.1 Cloud detection and preprocessing

Pixels flagged as cloud or snow are excluded from processing. The cloud masking technique used is configurable. The baseline implementation (Bevan et al., 2012) uses options for the AATSR supplied cloud flags with some additional tests. AATSR v2.1 products processed using Instrument Processing Facility version 6.01 (IPFv6.01) improve on the cloud tests of IPFv6.0 which were optimised for use over ocean (Zavody et al. 2000). The IPF improvements consist of applying a gross cloud test over land based on the 12 μm brightness temperature, disabling the spatial coherence test over land, and applying a test based on normalised difference indices using the visible channels (Birks 2007). To these tests further tests were added based on those described by Plummer (2008). Separate cloud masks for nadir and forward views are derived. A further option implemented is to perform a screening of cloud based on brightness, spectrum and temperature histograms, which was developed by FMI. Alternatively the method may read in an external cloud mask: for example, under CCI Common Cloud mask developed by DLR was implemented as an option in earlier tests.

In addition to the cloud mask a 'twilight zone' is implemented, where all pixels within a radius of *1* pixel of the original cloud mask are also labelled as cloud.

The surface is also classified into land or ocean to determine the algorithm which should be used. For glint over water bodies an additional test is used. This additional test makes use of the tabulated values of ocean BRF used for the ocean part of the aerosol retrieval. The LUT is used to estimate the ocean BRF in the 1.61um band for the viewing geometry of a given pixel assuming no AOD and a wind speed of 9m/s. Should the modelled ocean BRF exceed a threshold value the pixel is regarded as potentially glint contaminated and declared invalid.

5.1.1 Super-pixel aggregation

Although AATSR radiances are retrieved at a spatial resolution of 1km2, groups of 9 x 9 pixels are averaged before processing in order to reduce noise and minimise errors in coregistration between the forward and nadir images. The fraction of pixels in each 9 x 9 group required to be cloud free and of a given surface type is configurable. In the current version 75%, i.e. 61 of the 81 pixels need to cloud free or processing. The actual amount of available pixels per bin is reported by the algorithm and available in the output product.

Parameters such as geo-location, viewing geometry and acquisition time can therefore be directly inferred from the corresponding centre pixel. The geo-position and acquisition time of the super-pixel is defined to be the corresponding time of the nadir pixels.

Over land, for each pixel, both nadir and corresponding oblique pixels must be valid to accumulate that pixel within the super pixel aggregate, since the surface reflectance may be spatially homogenous. Over ocean the pixels aggregated to either nadir or oblique may be clear in that view only.

For a super-pixel to be valid the number of valid pixels in the bin needs to be evaluated separately for land and ocean. If more than 50% of either land or ocean pixels are valid the

super-pixel can be considered valid for retrieval. The spectral radiance of the super pixel is then represented by the arithmetic mean of the spectral radiances of the valid pixels. As the threshold is 50% a super-pixel can only be processed by either the land or ocean part of the retrieval. For dual view retrievals over land, both corresponding super-pixels need to be valid.

The result is a 'super-pixel' giving aggregated cloud-free TOA radiance for nadir and oblique view (if present) of the same surface location. Over ocean retrieval proceeds if either nadir or oblique super-pixels are valid (ie formed from at least 50% of valid pixels), while over land both nadir and oblique must be valid.

5.2 Aerosol model set

Pre-compiled LUTs for a set of candidate aerosol models are used to represent a range of aerosol types. For the baseline retrieval, the set comprised three fine-mode aerosol models (biomass burning, continental and urban) and two coarse-mode models (dust and sea salt) Vermote et al (1997). Under Aerosol CCI, the model set has been replaced by four aerosol types chosen to represent two coarse mode aerosol types (sea salt aerosol, desert dust) and two fine mode (weak absorbing, strong absorbing). While a continuous range of aerosol size distributions for these species exists (e.g. Nikonovas et al., 2015, 2017), intermediate size distrubtions are modelled by ratios of these end members. All assume spherical particles except for desert dust. Properties are listed in table 5.2-1. Optical properties were calculated using Mie code for the spherical particles, and T-matrix code for desert dust. The properties are fully documented in the *ESA Aerosol_cci Aerosol Model Technical Note*.

These models are used to form 35 mixtures of aerosol types by interpolation of properties (phase function, SSA) according to each 25% fraction within the total aerosol AOD. The Vector 6S code is then used to compute a LUT giving total column atmospheric radiative properties. In operation radiative properties for a continuous distribution of aerosol property variation (coarse/fine ratio, dust fraction etc.) are estimated by interpolation of properties defined at the LUT breakpoints.

Table 5.2-1: Optical Parameters for four CCI common aerosol models used. Log-normal parameters for two coarse and two fine mode aerosol components and their associated mid-visible refractive indices.

Aerosol component	Refr. index, real part (.55µm)	Refr. Index, imag part (.55µm)	reff (µm)	geom. st dev (σ_i)	variance (ln σ_i)	mode. radius (µm)
Dust	1.56	0.0018	1.94	1.822	0.6	0.788
sea salt	1.4	0	1.94	1.822	0.6	0.788
fine mode weak-abs	1.4	0.003	0.140	1.7	0.53	0.07
fine mode strong-abs	1.5	0.040	0.14	1.7	0.53	0.07

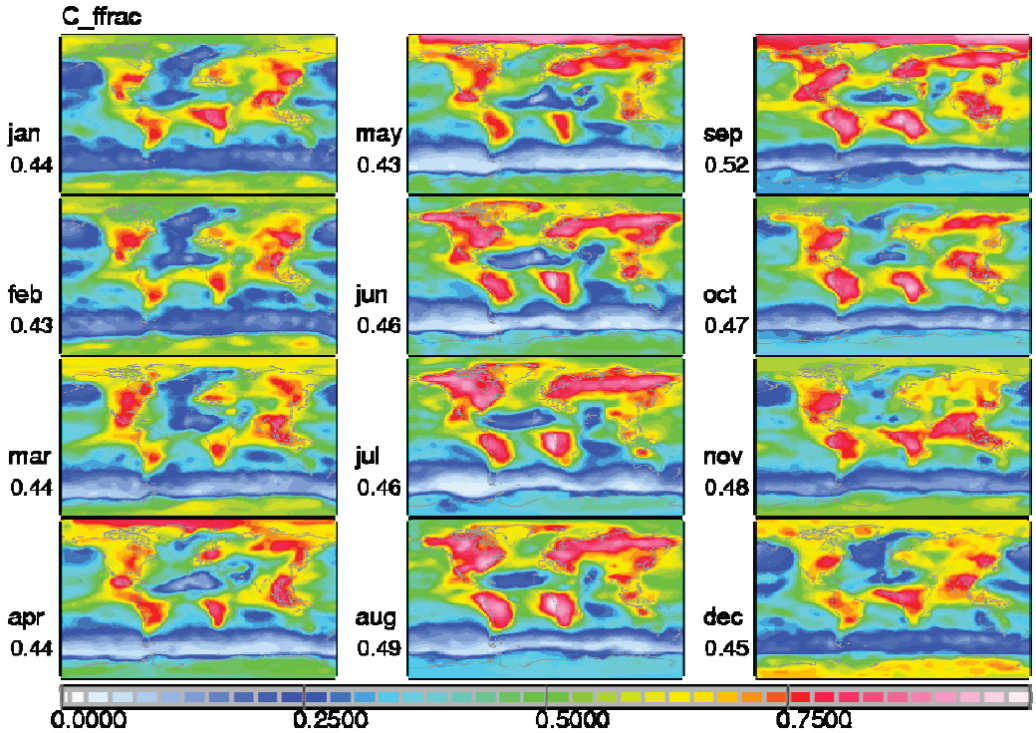

Figure 5.4-1: Example monthly climatology for fine mode fraction of total AOD at 550nm. Similar climatologies are used as input for dust fraction of coarse mode, and weakly absorbing fraction of fine mode AOD.

5.3 Aerosol climatology

The climatology of aerosol composition (Kinne et al., 2006) specifies mixing ratios of the four components on a 1° x 1° lat-long grid, separately for each of 12 months. The climatology is derived from merged model median estimates with data from AERONET; an example for fine mode fraction is shown in Figure 2. This is used to provide an a priori model of composition for aerosol retrieval, and allowing more robust estimation of properties of aerosol composition and absorption than possible to derive from the imagery alone. In operation, linear interpolation of the following are provided to the retrieval:

(i) Dust fraction of coarse mode AOD (550nm): Fdust

(ii) Weakly absorbing fraction of fine mode AOD (550nm): Fweak

(iii) Fine mode fraction of total AOD (550nm): FMF

Linear interpolation is used on lat/lon and month to provide an a priori estimate of each parameter per retrieval. The first two are used directly and not retrieved. However fine mode fraction of total AOD is used only as a default value – the fine mode AOD in the product is freely retrieved from the data.

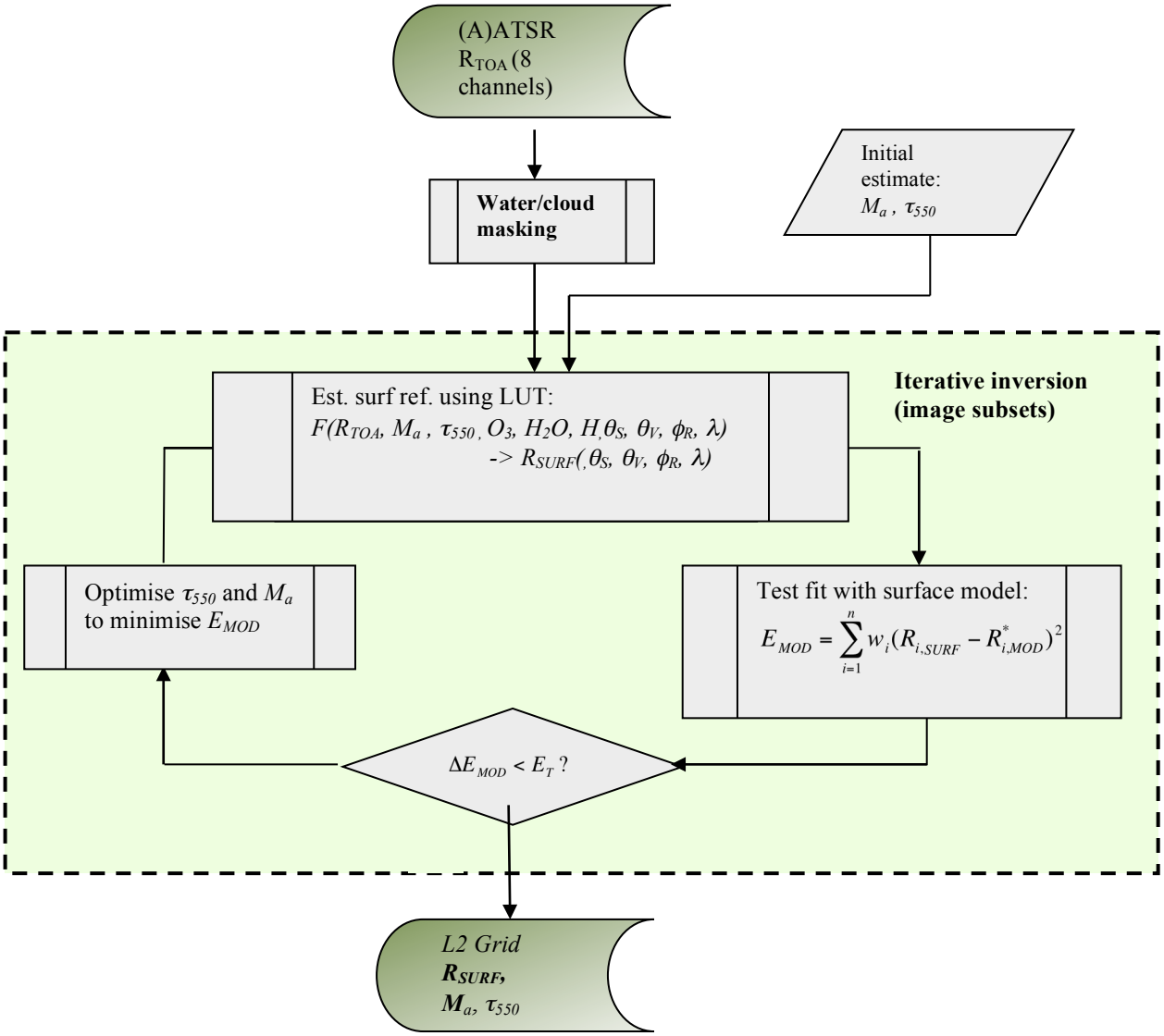

Figure 5.4-2: Overview of inversion scheme for retrieval of aerosol optical thickness at 550nm $\tau_{550}$and aerosol model M_a.

5.4 Atmospheric Look-Up Tables (LUTs)

Prior to operation a look-up table (LUT) is constructed to allow rapid run-time estimation of the quantities R_{atm}, T, R_{atm} by interpolation. In addition for the inversion we require a pre-computed estimate of $D(\theta_s)$ at each waveband, defined as the fraction of total downwelling light at the surface which is diffuse, defined at a fixed surface albedo (0.2). These quantities are pre-computed using the Vector 6S radiative transfer model (Vermote et al 1997; Kotchenova et al., 2007); however use of other accurate radiative transfer codes is possible.

In order to reduce computational cost we use Look Up Tables (LUT) of coefficients calculated by 6S in 4 dimensions. The dimensions are Aerosol Optical Thickness (AOT) at 550nm, relative azimuth angle (RAZ), view zenith angle (VZA) and solar zenith angle (SZA). The tie point set is detailed in Table 5.3-1. Each LUT entry contains values for each (A)ATSR waveband of the four coefficients required.

A set of LUTs is stored for each aerosol model. During operation we use multidimensional piecewise linear interpolation to obtain the required atmospheric coefficients for given solar/view geometry, waveband and AOT.

From the density of the lookup table grid points and the comparatively smooth behaviour of the TOA reflectance as a function of the LUT dimensions, we can estimate that the error introduced by the LUT approach and the employed linear interpolations is considerably smaller than the expected uncertainties due to selection of aerosol model parameters.

5.5 Inversion procedure

The input to the algorithm is the TOA product, averaged over a 10km x 10km window for each retrieval. This resolution is appropriate to minimise the effect of errors in image registration, while retrieving aerosol within the spatial scale of aerosol variability (North, 2002). The retrieval algorithm is outlined in figure 5.4-2.

Iterative inversion to minimise E_{MOD}, using the Brent one-dimensional minimisation gives an estimate of optical thickness and error of fit for a given aerosol model. The optimal aerosol model is selected by search for the aerosol model which minimises the estimated error from (6) or (7). Retrievals are run independently with different candidate models, and minimum value of E_{MOD} across the range of models provides an estimate for most likely aerosol type and corresponding properties of Angstrom coefficient, single scattering albedo and phase function.

While composition of dust / sea salt in coarse mode and weak / strong absorbing fine mode is determined by the above mentioned climatology, the retrieval determines aerosol size by running at 3 different sizes and fitting a parabola through Mein to determine the size fraction with optimal Mein. One of the three size fraction breakpoints is given by the climatology. If this fit of size fraction leads to results outside 0-1 the fraction reported by the climatology is used as fall back.

Table 5.3-1: Set of break points used for atmospheric look up table (LUT).

Parameter	Range	Interval	Number of breakpoints
RAZ	0 - 180°	20°	20
SZA	0 - 80°	5°	17
VZA			
- (A)ATSR nadir	0 - 25°	5°	6
- (A)ATSR forward	50-60°	5°	3
AOT (550 nm)	0-2	0.05	41

Summary of constraints employed in the retrieval

A set of practical constraints is included in the inversion to improve stability:

(i) After TOA -> SDR inversion:
for ocean: check for each channel / view if SDR()<-1e-3 then fmin = fmin + $(SDR)^2$*1000
if fmin > 100 skip retrieval
for land: check for each channel / view if SDR()<1e-3 then fmin = fmin + $(SDR-1e3)^2$*1000000
if fmin > 10 skip retrieval

(ii) Limits on the parameters within the land surface model are included within the Powell minimisation, by adding terms to the error fit (E_{mod}) to avoid unrealistic surface reflectance.:

$$if\ \ w(\lambda) < lim(\lambda)\ \ then\ Emod = Emod + 1000*(lim(\lambda) - w(\lambda))^2$$

where Iim = {0.03, 0.02, 0.01, 0.01 }

Stability is also found to be improved if the directional parameter $v(\Omega)$ is constrained to lie within a range close to 0.5 for the nadir view direction. The narrow range 0.49-0.51 is currently permitted:

$$if\ v<0.49\ then\ Emod = Emod + 1000*(0.49-v)^2$$
$$if\ v>0.51\ then\ Emod = Emod + 1000*(0.51-v)^2$$

While equivalent to a fixed value for v , expressing this as a constraint allows flexibility to optimise this parameter in future ATBD updates.

(iii) Constraint on fine mode fitting using Brent:

For CCI v43 the following constraint is used for the fitting of the fine mode fraction:

To ensure smoothness a weighted mean of the previously successfully retrieved fine mode values of the previous two lines and two columns (see Table 5.3-2) is computed :

$$prevFot = \Sigma(w_i * fot_i) / \Sigma w_i \quad (8)$$

Where fot_i is the fine mode fraction of the respective pixel and w_i are the weights computed as the inverse quadratic distance:

$$wi = 1 / ((x_i-x)^2 + (y_i-y)^2) \quad (9)$$

Table 5.3-2: Smoothness constraint weightings. Assuming processing lines first then if the orange is the current pixel, all green pixel cells should already have been processed. Hence these cells are considered for the computation of the previous fine mode fraction.

(x-2/y-2)	(x-1/y)	(x/y-2)	(x+1/y-2)	(x+2/y-2)
(x-2/y-1)	(x-1/y)	(x/y-1)	(x+1/y-1)	(x+2/y-1)
(x-2/y)	(x-1/y)	(x/y)	(x+1/y)	(x+2/y)
(x-2/y+1)	(x-1/y+1)	(x/y+1)	(x+1/y+1)	(x+2/y+1)
(x-2/y+2)	(x-1/y+2)	(x/y+2)	(x+1/y+2)	(x+2/y+2)

Initialisation of Brent and setting brackets:

1. Run Brent minimisation with climatology Fine Mode Fraction to determine upper AOD limit. Use the upper bracket (CX) of this Brent run for all subsequent AOD fits

2. Run Brent for fitting fine mode fraction with limits [0, 1] and starting point at climatology fine mode fraction.

3. Subsequently optimise for each fine mode fraction the AOD using [0, (CX)] as brackets and AOD starting point 0.05

5.6 Post-processing

The certain detection of cloud can be very challenging and perfect screening of cloud, especially optically thin clouds, is nearly impossible. However, even a very small or thin cloud can have strong impacts on the AOD retrieval. In the case of cloud contamination the AOD reported will be unreasonably high. The fact that clouds have a much larger spatial variability compared to typical aerosol distributions can be exploited to implement a post-processing step (Sogacheva et al., 2017).

The processing is a subsequent step after AOD retrieval has successfully finished for a larger region. It is a simple image processing considering all neighbours of a retrieved superpixel, i.e. boxes of 9 (3x3) superpixels. For an individual AOD retrieval to pass successfully this step of filtering the following criteria need to be met:

- at least 3 neighbouring superpixels with successful retrievals are required
- the sample corrected standard deviation of the valid superpixels in the 3x3 box need to be larger than 0.1

$$\sigma_\tau = \sqrt{\left(\frac{1}{N_{valid}-1}\sum_1^{N_{valid}}(\tau_i - \overline{\tau_i})^2\right)} < 0.1$$

5.7 EXPECTED ACCURACY

Accuracy has been evaluated empirically, based on overall comparison of retrieved products with AERONET and MAN, and varies with location and cover type. For the baseline product this is summarised in Bevan et al (2012) and for further versions within Aerosol_cci validation reports. However based on simulation studies (North 1999), the theoretical accuracy over land has been estimated as an absolute error in retrieval of aerosol opacity of the greater of 0.02 or 15% relative error over land surface for known aerosol model, and over ocean ~0.015 or 10% relative error. Results of validation and comparison with other satellite datasets are presented in de Leeuw et al. 2015 and Popp et al., 2016.

6 INPUT DATA REQUIREMENTS

The algorithm used as baseline AOT retrieval requires no external input data. The cloud masking procedure uses the static 0.25° IGBP land cover map within the Apollo algorithm. A version of the algorithm has also been implemented which makes use of a larger LUT to use available column ozone, water vapour and elevation data; however differences in retrieval were found to be small (<0.01 AOT at 550nm) for cases of elevation < 2km, and so the baseline algorithm as implemented on GPOD uses the simpler LUT with fixed values of 350 Dobson units for ozone, 3g cm^{-2} for water vapour and zero elevation.

7 ERROR BUDGET ESTIMATES

Over both land and ocean, the retrieval uses non-linear optimisation of an error function, of the form s the form

$$X^2 = \sum_{\lambda=1}^{\lambda=4} \sum_{\Omega=0}^{\Omega=55} \frac{(M(\lambda,\Omega) - O(\lambda,\theta))^2}{\sigma^2_{M(\lambda,\Omega)} + \sigma^2_{O(\lambda,\Omega)}} \tag{10}$$

where $\sigma_{M(\lambda,\Omega)}$ and $\sigma_{O(\lambda,\Omega)}$ denote estimates of 1 s.d. uncertainty in model and observation of surface reflectance at waveband λ and view direction θ (nadir is here denoted by θ=0°, forward view by θ =55°). It is possible to also include the full covariance matrix into the X^2 formulation, but currently error in model and observations are approximated as uncorrelated between channels.

For correctly normalised value of chi sq, the estimate of 1 s.d. error in τ_{550} is derived from the second derivative (curvature) of the error surface near the optimal value:

$$\sigma_{\tau 550} = \left(\partial^2 X^2 \big/ \partial^2 \tau_{550} \right)^{-0.5} \tag{11}$$

The curvature term is estimated by parabolic fit of the error function for surrounding values of τ_{550}.

Model error over land

Over land, model uncertainty was evaluated by inversion against the test dataset of surface BRDF values computed from a 3D Monte Carlo model. The 3D model and test dataset are described in North 1996 and North et al., 1999. Per channel errors were estimated from this fit as:

$$\sigma_{M\_land}(\lambda,\Omega) = \alpha_\lambda + \beta_\lambda M(\lambda,\Omega) \tag{12}$$

where

α={0.01, 0.01, 0.04, 0.02}
β={0}

No significant angular dependence of model error was found.

Model error over ocean

Over ocean the surface model is based on the models of Cox and Munk (1954) for glint, *Monahan & O'Muircheartaigh* (1980) and *Koepke* (1984) for foam fraction and spectral reflectance, and Morel's case I water reflectance model. Inputs required *a prori* are surface wind speed W (ms^{-1}) and pigment concentration C ($mg\ m^{-3}$).

Uncertainty in ocean reflectance model $M_{ocean}(\lambda,\Omega,W,C)$ is given by

$$\sigma^2_{M\_ocean} = \sigma^2_{M\_ocean\_W} + \sigma^2_{M\_ocean\_C} \quad (13)$$

where

$$\sigma_{M\_ocean\_W} = \left| M_{ocean}(\lambda,\Omega,W+\sigma_W,C) - M_{ocean}(\lambda,\Omega,W,C) \right|$$

$$\sigma_{M\_ocean\_W} = \left| M_{ocean}(\lambda,\Omega,W,C+\sigma_C) - M_{ocean}(\lambda,\Omega,W,C) \right|$$

Uncertainties in wind speed and pigment concentration are assigned values of 3 ms^{-1} and 0.1 mg m^{-3}

Observation errors

The per-channel observation error gives an estimate of the 1 s.d. uncertainty in derived land surface reflectance, and includes errors due to instrument calibration, radiative transfer model and LUT, and uncertainty in aerosol absorption parameterization.

$$\sigma^2_O = \sigma^2_{RT} + \sigma^2_{inst} + \sigma^2_{AerMod} \quad (14)$$

Approximations for these are given by:

$$\sigma^2_{inst} = T_S(\lambda,\theta)(a_\lambda + b_\lambda R_{TOA}(\lambda,\theta)), \quad (15)$$

where

$a = \{0.0005, 0.0003, 0.0003, 0.0003\}$
$b = \{0.024, 0.032, 0.02, 0.033\}$
this term is only implemented, a is neglected

The term Ts gives scaling from TOA to surface at

$$T_S(\lambda,\Omega) = \frac{\delta R_{SURF}(\lambda,\Omega)}{\delta R_{TOA}(\lambda,\Omega)} \quad (16)$$

and is derived from the LUT coefficients at time of inversion

Based on Kotchenova and Vermote (2007), error due to RT at all channels is approximated as

$$\sigma^2_{RT} = 0.006 \quad (17)$$

The error due to uncertainty in aerosol absorption is approximated by

$$\sigma_{AerMod} = 0.05 P_R(\lambda,\Omega) \quad (18)$$

where P_R denotes atmospheric path radiance, estimated from LUT values.

8 ALGORITHM OUTPUT

The algorithm output is the estimated AOT and best fitting aerosol model for each successful retrieval. The algorithm also outputs the uncertainty in AOD at 550nm., and surface reflectance at all solar reflective chanels. Further aerosol optical properties, such as Angstrom, may be derived based on those of the returned aerosol model. In addition, the algorithm performs a L3 monthly composite at 0.1 deg of aerosol AOT, modal aerosol type and surface reflectance. The output is summarised in table 8-1.

Table 8-1: Level 2 stripline products

Level 2 (stripline) products	Waveband	Spatial resolution
AOD for best-fit model	550 nm	10 km
Error (1 s.d.) in AOD	550 nm	
AAOD	550 nm	
AOD	659 nm	
Error (1 s.d.) in AOD		
AOD	865 nm	
Error (1 s.d.) in AOD		
AOD	1610 nm	
Error (1 s.d.) in AOD		
D_AOD	550 nm	
FM_AOD	550 nm	
Angstrom	550/865 nm	
SSA	550 nm	
Best-fit model properties:	550 nm	10 km
Ratio Coarse/fine (retrieved)		
Ratio Dust/sea salt (clim.)		
Ratio Weak/strong abs (clim)		
Nadir surface reflectance	550, 670, 870 and 1600 nm	1-10 km
	550, 670, 870 and 1600 nm	1-10 km
Applied cloud mask		1-10 km
Latitude		
Longitude		
Pixel corner latitude 1..4		
Pixel corner longitude 1...4		
Sun_zenith		
Satellite_zenith		
Relative azimuth		
Time		
Land sea flag		

9 PRACTICAL CONSIDERATIONS FOR IMPLEMENTATION

The algorithm is implemented in C. The code is modular, and uses pre compiled LUTs which may be readily changed to allow an arbitrary set of aerosol models. Timing shows a single daylight orbit typcially requires 20mins execution on a single processor 2.6Ghz Linux workstation. The code has been implemented at Swansea University on a Linux cluster with high number of cores (~400) to allow global processing of 1 year in ~48 hours. The code is also implemented at the UK CEDA facilit allowing direct access to (A)ATSR archive at UK PAC. Code verification has taken place between implementations by testing retrievals on a fixed dataset, and validation globally by automated comparison of AOT output with all available AERONET stations.

10 CONCLUSIONS

This report summarises the SU-ATSR algorithm Version 4.3, for retrieval of aerosol properties from the ATSR and AATSR instruments. Over land, the algorithm uses the AATSR dual-view capability to estimate aerosol without prior assumptions of land surface spectral properties. Over ocean the algorithm uses the low spectral reflectivity at red, near and mid infra-red channels to constrain aerosol retrieval using a priori estimates of wind speed and chlorophyll concentration. An analytic estimate of error in AOD is also made. In addition to AOD, we retrieve an aerosol model which gives an estimate of further aerosol properties. The data are produced both coincident with satellite overpass (Level 2) and as monthly composites (Level 3) at 0.1° resolution. Successful retrievals are possible over all regions, including bright desert surfaces, but excluding areas of sun glint, snow or cloud. Developments under the Aerosol CCI programme include (i) enhanced treatment of aerosol mixtures, (ii) inclusion of a model of ocean surface including wind-speed and pigment dependency, and (iii) analytical propagation of uncertainty.

REFERENCES

Bevan, S.L., North, P.R.J., Grey, W.M.F., Los, S.O. and Plummer, S.E. (2009), Impact of atmospheric aerosol from biomass burning on Amazon dry-season drought. *Journal of Geophysical Research*, **114**, D09204, doi:10.1029/2008JD011112.

Cox, C. and Munk, W. (1954). Statistics of the sea surface derived from sun glitter, *Journal of Marine Research,* **13**, 198-227.

Davies, W.H., North, P.R.J., Grey, W.M.F. and Barnsley, M.J. (2010), Improvements in Aerosol Optical Depth Estimation using Multi-angle CHRIS/PROBA Images, *IEEE Transactions on Geoscience and Remote Sensing,* **48**(1), 18-24.

Davies, W. & North, P. (2015). Synergistic angular and spectral estimation of aerosol properties using CHRIS/PROBA-1 and simulated Sentinel-3 data. *Atmospheric Measurement Techniques* 8(4), 1719-1731.

de Leeuw, G., Holzer-Popp, T., Bevan, S., Davies, W., Descloitres, J., Grainger, R. G., Griesfeller, J., Heckel, A., Kinne, S., Klüser, L., Kolmonen, P., Litvinov, P., Martynenko, D., North, P. J. R., Ovigneur, B., Pascal, N., Poulsen, C., Ramon, D., Schulz, M., Siddans, R., Sogacheva, L., Tanré, D., Thomas, G. E., Virtanen, T. H., von Hoyningen Huene, W., Vountas, M., & Pinnock, S., Evaluation of seven European aerosol optical depth retrieval algorithms for climate analysis, *Remote Sensing of Environment*, **2015**, *162*, 295 -315.

Grey, W.M.F., North., P.R.J., Los, S.O., and Mitchell, R.M., (2006). Aerosol optical depth and land surface reflectance from multi-angle AATSR measurements: Global validation and inter-sensor comparisons. *IEEE Transactions on Geoscience and Remote Sensing,* **44(8)**, 2184 – 2197.

Grey, W.M.F., North. P.R.J., and Los, S. (2006b). Computationally efficient method for retrieving aerosol optical depth from ATSR-2 and AATSR data, *App. Optics*, **45(12):** 2786-2795.

Kinne et al., (2006). An AeroCom initial assessment – optical properties in aerosol component modules of global models, *ACP*, **6**, 1-22.

Koepke, P. (1984). Effective Reflectance of Oceanic Whitecaps, *Applied Optics*, 23(11), 1816-1824.

Kotchenova, S.Y. and Vermote, E.F. (2007). Validation of a vector version of the 6S radiative transfer code for atmospheric correction of satellite data. Part II. Homogeneous Lambertian and anisotropic surfaces. *Applied Optics*, Vol. **46**, Issue 20, pp. 4455-4464.

Monahan, E.C. and O'Muircheartaigh, I. (1980). Optimal power-law description of oceanic whitecap dependence on wind speed, *Journal of Physical Oceanography*, **10**(12), 2094–2099, 1980.

Morel, A. (1988). Optical modeling of the upper ocean in relation to its biogenous matter content (case I waters), *Journal of Geophysical Research*, **93**(C9), 10749-10768, 1988.

Nikonovas, T., North, P. & Doerr, S. (2015). Smoke aerosol properties and ageing effects for northern temperate and boreal regions derived from AERONET source and age attribution. *Atmospheric Chemistry and Physics* 15(14), 7929-7943.

Nikonovas, T., North, P. & Doerr, S. (2017). Particulate emissions from large North American wildfires estimated using a new top-down method. *Atmospheric Chemistry and Physics (in press).*

North, P.R.J., Briggs, S.A., Plummer, S.E. and Settle, J.J., (1999). Retrieval of land surface bidirectional reflectance and aerosol opacity from ATSR-2 multi-angle imagery, *IEEE Transactions on Geoscience and Remote Sensing*, **37(1),** 526-537.

North, P. R. J. (2002). Estimation of aerosol opacity and land surface bidirectional reflectance from ATSR-2 dual-angle imagery: Operational method and validation, *J. Geophys. Res*., **107**, doi:10.1029/2000JD000,207.

North, P.R.J., Brockmann , C., Fischer, J., Gomez-Chova, L., Grey, W., Hecklel A., Moreno, J., Preusker, R. and Regner, P. (2008). MERIS/AATSR synergy algorithms for cloud screening, aerosol retrieval and atmospheric correction. *In Proc. 2nd MERIS/AATSR User Workshop, ESRIN, Frascati, 22- 26 September 2008.* (CD-ROM), ESA SP-666, ESA Publications Division, European Space Agency, Noordwijk, The Netherlands.

Popp, T., de Leeuw, G., Bingen, C., Brühl, C., Capelle, V., Chedin, A., Clarisse, L., Dubovik, O., Grainger, R., Griesfeller, J., Heckel, A., Kinne, S., Klüser, L., Kosmale, M., Kolmonen, P., Lelli, L., Litvinov, P., Mei, L., North, P., et. al. (2016). Development, Production and Evaluation of Aerosol Climate Data Records from European Satellite Observations (Aerosol_cci). *Remote Sensing* 8(5), 421.

Sobrino, J., Jiménez-Muñoz, J., Sòria, G., Ruescas, A., Danne, O., Brockmann, C., Ghent, D., Remedios, J., North, P., Merchant, C., Berger, M., Mathieu, P. & Göttsche, F. (2016). Synergistic use of MERIS and AATSR as a proxy for estimating Land Surface Temperature from Sentinel-3 data. *Remote Sensing of Environment* 179, 149-161.

Sogacheva, Larisa; Kolmonen, Pekka; Virtanen, Timo H; Rodriguez, Edith; Saponaro, Giulia; et al. (2017). Post-processing to remove residual clouds from aerosol optical depth retrieved using the Advanced Along Track Scanning Radiometer. Atmospheric Measurement Techniques 10.2: 491-505.

Vermote, E.F., Tanre, D., Deuze, J.L., Herman, M. and Morcrette, J.J. (1997). Second simulation of the satellite signal in the solar spectrum, 6S: An overview, *IEEE Trans. Geosci. Remote Sensing* **35**, pp. 675–686.

End of the document